

This article was downloaded by:

On: 23 January 2011

Access details: *Access Details: Free Access*

Publisher *Taylor & Francis*

Informa Ltd Registered in England and Wales Registered Number: 1072954 Registered office: Mortimer House, 37-41 Mortimer Street, London W1T 3JH, UK



## Journal of Carbohydrate Chemistry

Publication details, including instructions for authors and subscription information:

<http://www.informaworld.com/smpp/title~content=t713617200>

### Structure and Conformation of Mannoamidines by Nmr and Molecular Modeling: are They Good Transition State Mimics?

Yves Blériot<sup>a</sup>; Arnaud Genre-Grandpierre<sup>a</sup>; Anne Imberty<sup>b</sup>; Charles Tellier<sup>a</sup>

<sup>a</sup> Unité de Recherche sur la Biocatalyse, <sup>b</sup> Laboratoire de Synthèse Organique Sélective, URA n 475 Faculté des Sciences et des Techniques, France

**To cite this Article** Blériot, Yves , Genre-Grandpierre, Arnaud , Imberty, Anne and Tellier, Charles(1996) 'Structure and Conformation of Mannoamidines by Nmr and Molecular Modeling: are They Good Transition State Mimics?', *Journal of Carbohydrate Chemistry*, 15: 8, 985 – 1000

**To link to this Article:** DOI: 10.1080/07328309608005704

**URL:** <http://dx.doi.org/10.1080/07328309608005704>

PLEASE SCROLL DOWN FOR ARTICLE

Full terms and conditions of use: <http://www.informaworld.com/terms-and-conditions-of-access.pdf>

This article may be used for research, teaching and private study purposes. Any substantial or systematic reproduction, re-distribution, re-selling, loan or sub-licensing, systematic supply or distribution in any form to anyone is expressly forbidden.

The publisher does not give any warranty express or implied or make any representation that the contents will be complete or accurate or up to date. The accuracy of any instructions, formulae and drug doses should be independently verified with primary sources. The publisher shall not be liable for any loss, actions, claims, proceedings, demand or costs or damages whatsoever or howsoever caused arising directly or indirectly in connection with or arising out of the use of this material.

**STRUCTURE AND CONFORMATION OF MANNOAMIDINES  
BY NMR AND MOLECULAR MODELING :  
ARE THEY GOOD TRANSITION STATE MIMICS ?**

Yves Blériot,<sup>a,c</sup> Arnaud Genre-Grandpierre,<sup>a</sup> Anne Imberty<sup>b</sup>  
and Charles Tellier\*<sup>a</sup>

a) Unité de Recherche sur la Biocatalyse,

b) Laboratoire de Synthèse Organique Sélective, URA n 475  
Faculté des Sciences et des Techniques, 2, rue de la Houssinière  
44072 Nantes cedex 03, France

c) Present address: Dyson Perrins Laboratory, South Parks Road  
Oxford, OX1 3QY, U.K.

*Received February 23, 1996 - Final Form July 23, 1996*

**ABSTRACT**

The conformation of two mannose-based amidines, the *N*-benzylmannoamidine and a pseudo (1→6) dimannoside, has been evaluated using semi-empirical AM1 calculations and <sup>1</sup>H NMR studies. The most stable conformations of the mannoamidine ring correspond to the half-chair forms <sup>3</sup>H<sub>4</sub> and <sup>4</sup>H<sub>3</sub>. The conformations (*Z*) or (*E*) about the exocyclic C-N bond depend on the substituents and it was shown that, in solution, the *N*-benzylmannoamidine was (*E*)-configured whilst the pseudo (1→6) dimannoside was (*Z*)-configured. Using the grid-search approach, the potential energy maps of both mannoamidines were calculated as a function of the torsion angles which define the orientation of the amidine substituent. Three stable conformers were identified for the *N*-benzylmannoamidine and seven for the pseudo (1→6) dimannoside. Inter-glycosidic NOE have provided evidence for a preferred conformation of the pseudo (1→6) dimannoside in solution. The transition state structure of the α-phenylmannose hydrolysis was optimized using the AM1 method and compared to the *N*-benzylmannoamidine. The developing oxocarbenium ion is well matched by the mannoamidine ring but the orientation of the phenyl group in the inhibitor differs significantly from the position of the leaving group in the transition state. The use of sugar type amidines as haptens to obtain catalytic antibodies is then discussed.

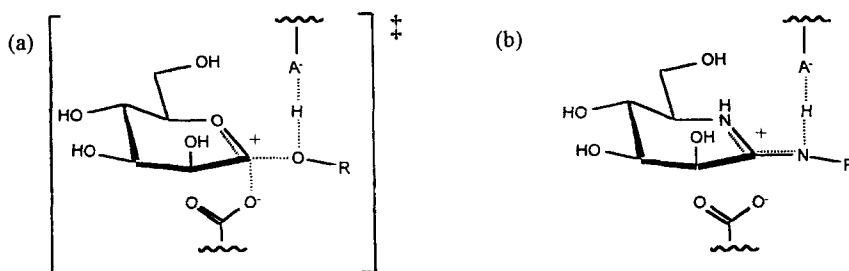


**Figure 1.** Schematic representation of (a) the transition state in the hydrolysis of a  $\beta$ -mannoside and (b) the probable binding mode of a protonated amidine with the active site catalytic residues of a glycosidase.

## INTRODUCTION

Amidine derivatives of sugars have been recently synthesized<sup>1</sup> and been shown to be potent inhibitors of glycosidases ( $K_i = 10^{-5}$ - $10^{-8}$  M).<sup>2</sup> The efficiency of these inhibitors has been related to their structure which is thought to mimic the flattened chair conformation and the positive charge of the transient glycosyl cation in a glycosidase mechanism (Figure 1). Enzymic-catalyzed glycoside hydrolysis is believed to proceed *via* the protonation of the exocyclic anomeric oxygen atom by an acidic residue of the active site, followed by the slow cleavage of the O-1-C-1 bond, to generate a cyclic oxocarbenium ion. Attack by water then results in the formation of the free sugar.<sup>3</sup>

The apparent structural similarity between the transition state of the glycoside hydrolysis and the amidine derivatives has suggested to us and others<sup>4</sup> the use of these molecules as transition state analogues to generate catalytic antibodies.<sup>5</sup> In this approach, it was assumed that: (i) the half-chair conformation of the amidine would generate a binding site in the antibody that would distort the mannose ring from its normal chair conformation and so aid the aglycon departure; (ii) the amidine positive charge would induce a complementary charge in the binding site, presumably as a carboxylate group, that would either act as a proton donor to the exocyclic anomeric oxygen or stabilize the oxocarbenium ion during the time course of the hydrolysis; (iii) the presence of a hydrophobic substituent in the amidine would generate a hydrophobic pocket in the "aglycon" binding site in order to avoid product inhibition. Until now, such amidine-based haptens failed to elicit any catalytic activity among the numerous high affinity monoclonal antibodies which have been produced.

We show that information obtained from  $^1\text{H}$  NMR and molecular modeling studies helps to understand the structure and the conformation of sugar derived amidines. Their similarity with the transition state of glycoside hydrolysis is then discussed, based on this conformational analysis.

## RESULTS AND DISCUSSION

**Conformation of the mannoamidine ring.** We carried out semiempirical calculations on *N*-benzylmannoamidine **1** and the pseudo (1 $\rightarrow$ 6) dimannoside **2** (Figure 2) that we previously synthesized.<sup>6,7</sup> The AM1 method<sup>8</sup> was used for systematic conformational searches and molecular geometries were fully optimized without any constraints. Only protonated species of these amidine-based sugars were considered for the calculations as they predominate at neutral pH ( $\text{pK}_a > 9$ ).<sup>9</sup> Although protonation of a cyclic amidine can occur either at the N-5' or the N-1' site leading to different tautomers, AM1 calculations on the resulting species indicate that the amidine protonates essentially at the imino nitrogen to give the conjugate acid.<sup>10</sup> This amidinium ion with a delocalized positive charge adopts a half-chair conformation with a bond order  $> 1$  for the N-5'—C-1' and C-1'—N-1' bonds.

Considering the mannoamidine ring, we found four minima corresponding to half-chair conformations where atoms C-2', C-1', N-1', N-5' and C-5' are nearly co-planar. These minima correspond to the two possible half-chair conformations  $^3\text{H}_4$  and  $^4\text{H}_3$  combined with the (*Z*)-, (*E*)-stereoisomers at the C-1'—N-1' bond as defined in Table 1. Only structures with the (*E*)-isomer of the C-1'—N-5' bond were considered, since only this stereochemistry is sterically accessible to the cyclic amidine. For both compounds the most stable form is the isomer *EZ*,  $^3\text{H}_4$  at the AM1 level.

The  $^3\text{H}_4$  conformation is preferred over the  $^4\text{H}_3$  conformation. Changing the stereochemistry at the C-1'—N-1' bond from the (*Z*) to the (*E*) form increases the energy by 3.5 kcal/mol. The preference for the (*Z*)-isomer is consistent with previous calculations obtained for other amidines and crystal structure of cyclic amidines.<sup>11</sup> However, AM1 calculations are more appropriate to gas phase and experimental results on simple amidinium ions have shown that the equilibrium between the (*E*) and (*Z*) isomers is strongly dependent on the solvent and the counterions.<sup>11</sup>

To address this problem, we used  $^1\text{H}$  NMR coupling constants and NOE data for the analysis of the conformation of these amidine-based sugars.  $^1\text{H}$  chemical shifts for **1** and **2** were obtained from the COSY spectrum and are collected in Table 2 together with the corresponding  $^3J_{\text{H-H}}$  coupling constants. For the mannoamidine ring, theoretical

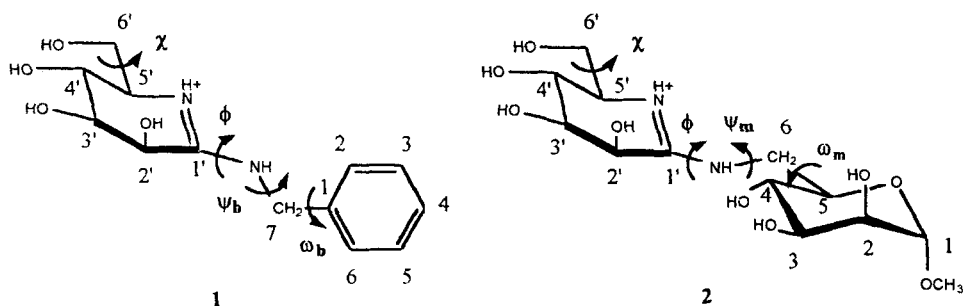
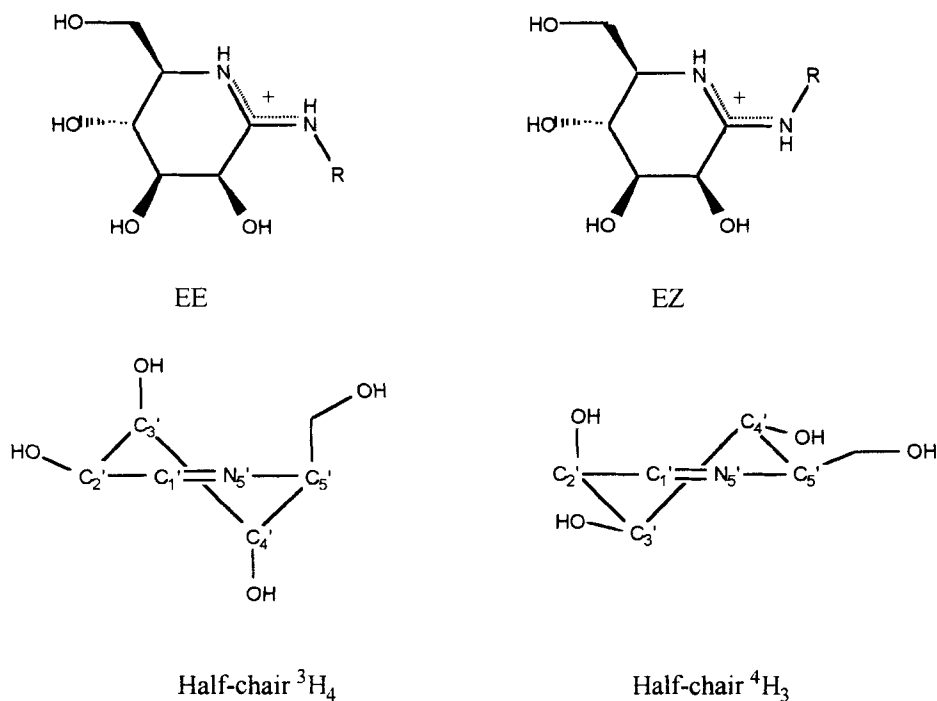


**Figure 2.** Schematic representation of the benzylmannoamidinium (1) and the pseudodimannoside (2), with the labelling of the atoms and structural descriptors of interest ( $\chi = \Theta(\text{N-5}'\text{-C-5}'\text{-C-6}'\text{-O-6}')$ ,  $\phi = \Theta(\text{N-5}'\text{-C-1}'\text{-N-1}'\text{-C-x})$ ,  $\psi_b = \Theta(\text{C-1}'\text{-N-1}'\text{-C-7-C-1})$ ,  $\omega_b = \Theta(\text{N-1}'\text{-C-7-C-1-C-2})$ ,  $\psi_m = \Theta(\text{C-1}'\text{-N-1}'\text{-C-6-C-5})$ ,  $\omega_m = \Theta(\text{N-1}'\text{-C-6-C-5-O-5})$ ).

values calculated from Altona's empirical equation<sup>12</sup> for the two half-chair conformations are also reported in Table 2. The comparison between the calculated and the observed values provides evidence for a rapid exchange between the <sup>3</sup>H<sub>4</sub> and <sup>4</sup>H<sub>3</sub> forms in solution which gives motional averaged chemical shift values. The experimental *J* values give also evidence that the energetic advantage of the <sup>3</sup>H<sub>4</sub> deduced from the AM1 calculations is far less important in solution. The proportion of <sup>3</sup>H<sub>4</sub> and <sup>4</sup>H<sub>3</sub> forms in solution seems to be almost equal. Those discrepancies could arise from the difficulty of the AM1 method to provide accurate energy.<sup>13</sup>

Because the preference for stereoisomer (*E*) or (*Z*) can be affected by the solvent or the amidine counterions, we have used a conformational analysis of the sugar based amidine 1 and 2 in D<sub>2</sub>O solution using the Nuclear Overhauser Effect. In D<sub>2</sub>O at room temperature, both amidinium ions seem to exist as only one conformer as revealed by the absence of splitting of NMR lines. A mixture of both conformers should give additional peaks since *E* isomer resonances are generally downfield of *Z* resonances, as in amide.<sup>11</sup> If the preferred conformer were (*EZ*), a strong NOE would be expected between the protons H-2' and H-7 in compound 1 and between H-2' and H-6a, H-6b in compound 2. The calculated distances based on molecular modeling studies lie between 2.5 Å and 3.2 Å. On the other hand, if the preferred isomer is (*EE*), no strong NOE is expected with proton H-7 (1) and H-6 (2) since H-5' exchanges with deuterium in D<sub>2</sub>O. In the NOESY spectrum (data not shown) a positive intra-residue NOE is detected between proton pairs H-2'-H-3' and H-2'-H-5', and an inter-residue NOE is clearly visible between H2' and H7

**Table 1 :** Structural and energetic characteristics of different conformers of structures **1** and **2** deduced from semiempirical calculations with AM1.  $\Delta\Delta H_f$  is expressed in kcal/mol and represents the relative AM1 heat of formation. Dihedral angles  $\chi$ ,  $\Phi$ ,  $\Psi$ ,  $\omega$  are defined in Fig. 2 and are expressed in  $^\circ$ . For geometric optimisation, starting orientation of the hydroxymethyl group 6' corresponds to the more stable *GT* orientation ( $\chi \sim 60^\circ$ ).



Compound	Conformer	$\Delta\Delta H_f$	$\chi$	$\phi$	$\psi$	$\omega$
1	<i>EZ</i> , ${}^3H_4$	0	52.7	4.2	168.5	-98.2
1	<i>EZ</i> , ${}^4H_3$	3.4	54.4	2.4	170.6	-104.8
1	<i>EE</i> , ${}^3H_4$	3.5	52.7	-171.1	165.4	86.4
1	<i>EE</i> , ${}^4H_3$	5.1	55.2	177.9	-173.9	78.8
2	<i>EZ</i> , ${}^3H_4$	0	54.8	2.7	-159.7	166.9
2	<i>EZ</i> , ${}^4H_3$	2.8	55.4	2.4	-172.9	171.2
2	<i>EE</i> , ${}^3H_4$	3.5	54.7	-166.9	168.4	175.6
2	<i>EE</i> , ${}^4H_3$	4.5	55.7	-178.5	-170.4	172.1

**Table 2** : 400 MHz  $^1\text{H}$  chemical shifts (ppm) and observed  $^3J_{\text{H-H}}$  coupling constants (Hz) for compounds **1** and **2**.

proton	$\delta$ (ppm)	exptl $J$ (Hz)	calc $J$ ( $^3\text{H}_4$ ) <sup>a</sup>	calc $J$ ( $^4\text{H}_3$ ) <sup>a</sup>
<b>benzylmannoamidinium 1</b>				
H-2' ( $J_{\text{H-2}'-\text{H-3}'}$ )	4.76	3.5	3.3	4.0
H-3' ( $J_{\text{H-3}'-\text{H-4}'}$ )	4.12	3.7	3.2	9.7
H-4' ( $J_{\text{H-4}'-\text{H-5}'}$ )	3.90	5.7	0.8	9.4
H-5' ( $J_{\text{H-5}'-\text{H-6'a}}$ )	3.42	5.9	11.1	11.2
( $J_{\text{H-5}'-\text{H-6'b}}$ )		4.3	3.9	3.9
H-6'a, H6'b ( $J_{\text{H-6'a}-\text{H-6'b}}$ )	3.67, 3.82	11.9		
<b>pseudo-dimannoside 2</b>				
H-2' ( $J_{\text{H-2}'-\text{H-3}'}$ )	4.22	3.7	3.5	4.0
H-3' ( $J_{\text{H-3}'-\text{H-4}'}$ )	~ 3.99	n.d	3.1	9.6
H-4' ( $J_{\text{H-4}'-\text{H-5}'}$ )	~ 3.99	5.8	0.9	9.3
H-5' ( $J_{\text{H-5}'-\text{H-6'a}}$ )	3.59	6.9	11.1	11.1
( $J_{\text{H-5}'-\text{H-6'b}}$ )		4.2	3.8	3.9
H-6'a, H6'b ( $J_{\text{H-6'a}-\text{H-6'b}}$ )	3.86-4.03	11.6		

<sup>a</sup> Calculated  $J$  values were obtained from the Altona and Haasnoot equation.<sup>12</sup>

protons consistent with the presence of an (*EE*) stereoisomer for **1**. Similar experiment with compound **2** failed to detect any NOE between protons H-2' and H-6a or H-6b suggesting that the (*EZ*) form is preferred which is in agreement with semi-empirical calculations. The preference for the (*EE*) form of **1** can be rationalized in terms of the electron-withdrawing properties of the substituents. It has been observed that electron-donating substituents shift the equilibrium towards the (*EZ*) form, whereas electron-withdrawing substituents can delocalize the lone pair on the nitrogen and stabilize the (*EE*) form, as observed with the benzyl substituent in **1**.<sup>11</sup>

**Orientation of the primary hydroxyl groups.** The preferred orientation of the primary hydroxyl group of the mannoamidinium ring was determined by AM1 calculation for the four preferred isomers. The results of the energy calculation as a function of the torsional angle  $\chi$  indicate that whatever the isomers, the *gauche-trans* (*GT*) position is preferred. The population of the three rotamers *gauche-gauche* (*GG*), *gauche-trans* (*GT*), and *trans-gauche* (*TG*) was calculated from the relaxed energy minima of each rotamer. For the benzylmannoamidinium with  $^3\text{H}_4$  conformation, the *GT* rotamer represents more than

95 % of the population ( $GG : GT : TG = 0.3 : 95.0 : 4.7$ ). For the  ${}^4H_3$  conformer, the  $GT$  rotamer is still preferred but the abundance of  $GG$  rotamer increases ( $GG : GT : TG = 11.2 : 86.2 : 2.6$ ). This preference for the  $GT$  rotamer has also been demonstrated in standard glycosides.<sup>14</sup>

Experimental validation of these calculations could in principle be obtained from the measurement of H-5'-H-6'S and H-5'-H-6'R coupling constants. However, as the NMR time scale is slower than the internal reorientation in molecules, the observed values correspond to an average structure taking all the possible conformations using a Boltzman distribution. Another difficulty would be the differentiation of the two prochiral protons.

**Inter-residue conformation.** For each compounds **1** and **2**, a conformational analysis of the orientation of the amidine substituent was performed using AM1 energy calculation. Figures 3 and 4 represent the potential energy map of compounds **1** and **2** and thus were obtained by systematic increment of the torsional angle  $\psi$  and  $\omega$  which determine the inter-residue conformation. The orientation of the hydroxymethyl group was fixed to the more stable  $GT$  rotamer.

For benzylmannoamidine **1**, the rigid potential energy surfaces identified three main energy minima domains corresponding to different orientations of the benzyl group relative to the mannoamidine ring. The calculation of a "relaxed" energy map where a geometry optimisation is performed for each  $\psi$  and  $\omega$  torsional angle was impossible due to the computation time needed for such a study. However, force field calculations on disaccharides have demonstrated that "relaxed" maps are consistent with rigid map in terms of the overall shape and the location of the minima.<sup>15</sup> Nevertheless, the lowest energy conformations of each domain were submitted to full optimization and yielded to the three conformers A1, A2 and A3 that are represented in Figure 3. The calculated energies and the corresponding torsion angles  $\psi_b$  and  $\omega_b$  are reported in Table 3 and show that the global minimum corresponds to an extended conformation of the residues. Interestingly, two other conformers with a slightly higher energy were detected that corresponding to the benzyl group being located above (A2) or below (A3) the mannoamidine ring.

For the pseudo (1→6) dimannoside **2**, up to seven low energy domains were identified on the "rigid" energy map (Figure 4) and their relative energies are reported in Table 3.

It appears that the conformational space that can be experienced by this disaccharide is larger than that of the corresponding natural disaccharide, Man  $\alpha(1-6)$



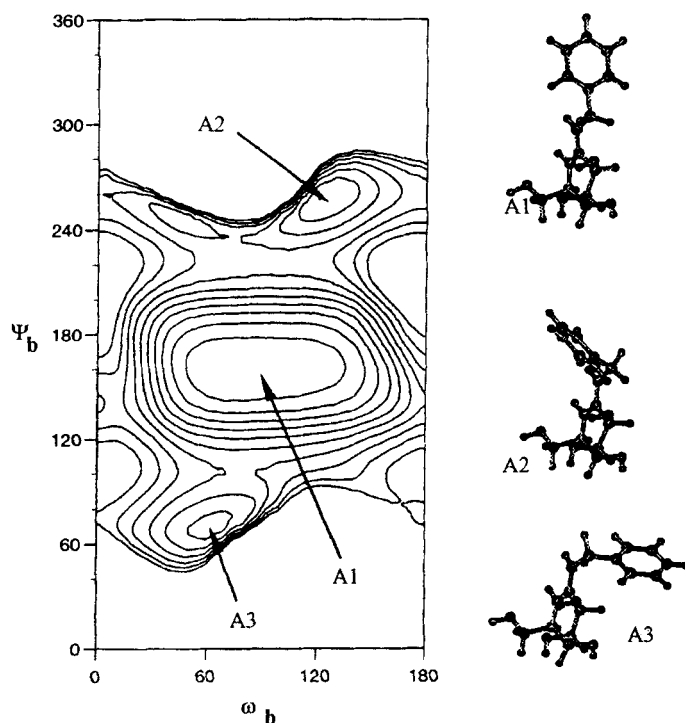


**Figure 3.** Potential energy map of the benzylmannoamidine **1** as a function of the  $\psi_b$  and  $\omega_b$  torsion angles. The hydroxymethyl group was fixed in the preferred *GT* orientation and the *EE*,  $^3H_4$  conformer of the amidine ring was used. Isoenergy contours are drawn at increments of 1 kcal/mol with respect to the absolute minimum. The three low energy conformers are labelled A1, A2 and A3 and are represented as stick and ball models.

Man.<sup>16</sup> This increased flexibility of compound **2** can be explained by the planar structure of the amidinium part, which puts the two residues away from each other, thus avoiding steric conflict between the residues. For these reasons, inter-residue hydrogen bonds are only possible in the low energy conformers B4.

Experimental informations about pseudo-(1→6) dimannoside **2** conformations in solution were obtained from the inter-residue NOE volumes. Figure 5 shows the sum of the NOESY slices at the H-2' frequency where three inter-residue NOEs were detected between protons H-2' and H-1, H-2' and CH<sub>3</sub>, and H-2' and H-5. The low-energy conformer where in the calculated inter-proton distances would agree with the observed NOE corresponds to conformer B3 (Fig. 5). This conformer is one of the lowest energy conformers (Table 3) detected by AM1 calculations. All other conformers failed to

**Table 3:** Relative energies and geometrical features of the stable conformers of **1** and **2** after complete geometry optimisation.

name	Relative <sup>a</sup> energy	$\psi$	$\omega$	possible hydrogen bond
benzylmannoamidine				
A1	0	165.4	86.4	
A2	1.46	-105.3	115.4	
A3	1.68	68.9	67.8	
pseudo-dimannoside				
B1	0	76.5	-72.3	
B2	0.16	-93.7	-58.7	
B3	0.95	-82.5	-65.7	
B4	1.65	68.8	101.2	N-5'---O-4
B5	2.07	-175.	-53.	
B6	2.64	-159.7	166.9	
B7	2.66	175.8	60.8	

<sup>a</sup> relative energy expressed in kcal/mol

explain simultaneously the observed NOE indicating that the main pseudo-(1→6) dimannoside conformation is close to the conformer B3 in solution.

**Comparison with the transition state of glycoside hydrolysis.** The strong competitive inhibition of various glycosidases by amidine-based sugars has suggested that amidines could behave as transition state analogues of glycoside hydrolysis.<sup>1</sup> This hypothesis could in principle be tested by kinetic measurements of the correlation between the  $K_i$  of a series of inhibitors and the  $K_m/k_{cat}$  of the corresponding substrates.<sup>17</sup> This correlation is difficult to establish because glycosidases do not permit extensive substrate variation and consequently do not have a broad range of  $K_m/k_{cat}$ .

The alternative is to combine inhibitor analogues and variation of enzyme structures,<sup>18</sup> but this approach implies the availability of various mutants of the same enzyme.<sup>19</sup> Recent pH dependent studies have shown that it is the protonated form of the amidines which binds to the glycosidase and that these inhibitors bind to a protonation states of glycosidases different from that required for catalysis.<sup>2b</sup> This suggests that tight binding does not necessarily establish mimicry of the transition state.

Previous conformational analysis of the amidine-based sugars **1** and **2** can help to understand the difference between these inhibitors and the putative transition state of

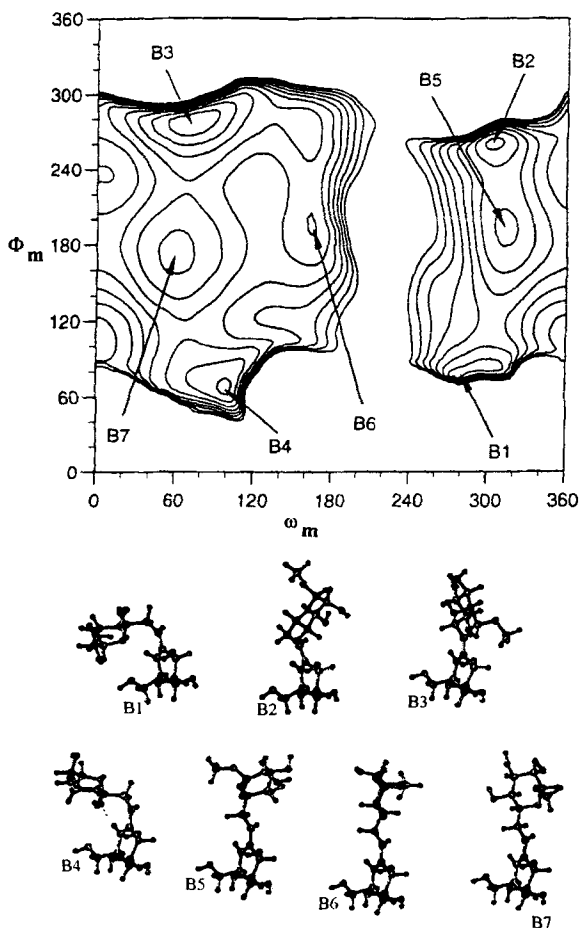


**Figure 4.** Potential energy map of the pseudo-(1→6) dimannoside **2** as a function of the  $\psi_m$  and  $\omega_m$  torsion angle. The hydroxymethyl group was fixed in the preferred *GT* orientation and the *EZ*, $^3H_4$  conformer of the amidine ring was used. Isoenergy contours are drawn at increments of 1kcal/mol with respect to the absolute minimum. The seven low energy conformers are labelled B1-B7 and are represented as stick and ball models. Interresidue hydrogen bond are drawn with dotted lines.

glycoside hydrolysis. The geometry and the partial charge of the transition state of the acid hydrolysis of phenyl- $\alpha$ -D-mannose were calculated using semi-empirical methods. It has been shown that structural characteristics of the transition state obtained with semi-empirical calculations are close to the structure obtained by *ab initio* calculation.<sup>20</sup> In Table 4, selected bond lengths and partial atomic charges of the amidinium salt **1** are compared with the corresponding substrate in the ground state and transition state. This

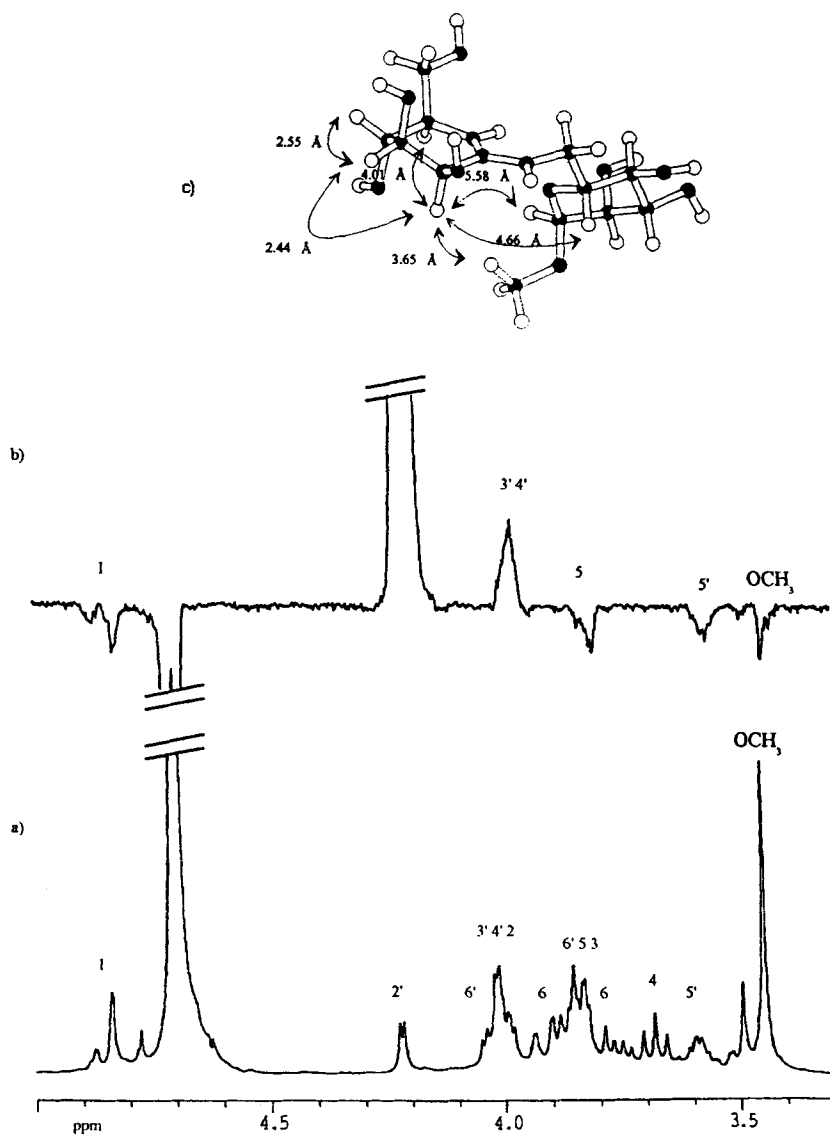


**Figure 5.** 400 MHz <sup>1</sup>H NMR spectra of the pseudo-(1→6) dimannoside **2**. a) one-dimensional spectrum of **2**. b) one-dimensional NOESY subspectrum at H-2' frequency where NOEs are observed. c) structure of the conformer B3 with the inter-proton distances within the parenthesis.

**Table 4:** Selected structural parameters of phenyl- $\alpha$ -D-mannoside in the ground state (GS), in the transition state (TS) and benzyl-mannoamidinium **1** obtained from semi-empirical calculations.

	GS	TS	<b>1</b>
bond lengths:			
<sup>a</sup> X-5'-C-1'	1.41	1.31	1.35
C-1'-X-1'	1.42	1.89	1.35
partial charges: <sup>b</sup>			
X-5'	-0.353	-0.204	-0.042 <sup>c</sup>
C-1'	+0.250	+0.367	+0.357
X-1'	-0.289	+0.006 <sup>c</sup>	-0.049 <sup>c</sup>
torsion angles:			
C-5'-X-5'-C-1'-X-1'	62.5	85.3	-177.8
X-5'-C-1'-X-1'-C	101.8	105.8	177.9
bond angle:			
X-5'-C-1'-X-1'	106.1	91.9	121.6

<sup>a</sup> X refers to an oxygen atom in the GS and TS structures and a nitrogen atom in **1**.

<sup>b</sup> partial charges obtained from MNDO calculations.

<sup>c</sup> Partial charges corresponding to the protonated heteroatom (XH).

shows that the amidinium ring closely resembles the oxocarbenium ion in terms of geometry and partial atomic charges, indicating that amidinium ring is a good mimic of oxocarbenium ion.

However, the position of the exocyclic NH in amidines is very different from that of the protonated oxygen in the transition state. In the latter, the trigonal planar geometry at C-1' places the departing aglycon-C-1' bond at approximately 90° (Table 4) from the plane defining the oxocarbenium ion. The sp<sup>2</sup> hybridization at C-1' in the inhibitors leaves the exocyclic NH in the mannoamidinium plane. As a result, the substituted amidines do not fit correctly the position of the leaving group in the acetal hydrolysis (Figure 6). In transition state structure, the phenyl group is located above or below the oxocarbenium ion depending on whether the starting configuration was  $\alpha$  or  $\beta$ , whereas in mannoamidinium **1**, the benzyl group is extended away from the mannoamidinium ring in the global minimum. Secondary minima detected by conformational analysis placed the benzyl group in a position similar to the departing phenol in the transition state but not exactly in the same plane. As these conformers have energy close to the global minimum, it is conceivable that enzyme could bind these conformers without too much binding cost.

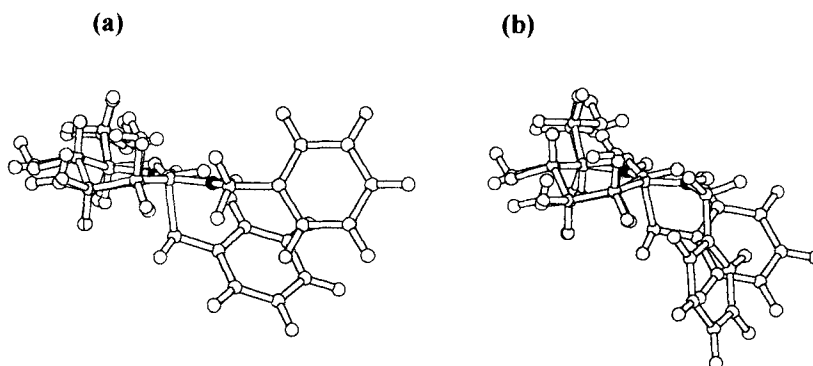


**Figure 6.** Comparison of aglycon positioning for the transition state of phenyl- $\alpha$ -D-mannoside hydrolysis and the benzylmannoamidine 1 inhibitor. The superimposed structures are obtained by placing the oxocarbenium and the mannoamidine ring in isosteric conformation. (a) superposition of the transition state and of the more stable conformer B1 of 1. (b) superposition of the transition state and the local energetic minimum B3 which places the phenyl ring in a conformation near that of the transition state.

**Conclusion.** Molecular modeling and  $^1\text{H}$  NMR studies have demonstrated that amidine-based sugars are not perfect mimics of the transition state of glycosides when they have been hydrolysed. These enzymes accelerate hydrolysis of glycoside bond by a factor  $> 10^{14}$  relative to the uncatalyzed reaction in water at neutral pH.<sup>3</sup> According to the transition state theory, a perfect transition state analogue that could generate catalytic antibodies with glycosidase activity should have a  $K_i < 10^{-16}$  M since most of the  $K_m$  ( $K_s$ ) are in the range 0.1 to 10 mM. The best inhibition observed with the amidine-based sugars are in the  $10^{-8}$  M range, and are therefore far from a perfect transition-state analogue. Hence the best catalytic antibodies that could be expected using standard strategy of production would have low efficiency ( $k_{\text{cat}}/k_{\text{uncat}} = K_m/K_i < 10^6$ ). This rate of acceleration is too low to allow detection of catalytic antibodies and kinetic analysis on non-activated glycosides. For these reasons, we and others<sup>4</sup> tried to elicit catalytic antibodies against cyclic amidines that would be capable of hydrolysing acetal bonds with a lower energy barrier for hydrolysis as in aryloxytetrahydropyran ( $k_{\text{uncat}} = 10^{-3} \text{ min}^{-1}$ ). The failure of this approach can be rationalized with the present structural studies. On one hand, the most stable conformations of substituted cyclic amidine are far from the transition-state and the ground state of the corresponding glycoside and therefore good amidine binder antibodies would not be able to bind the substrate. Accordingly, among six monoclonal antibodies which were selected to strongly bind

amidine as hapten ( $K_d = 10^{-6}$ - $10^{-8}$  M), none of them were able to bind the corresponding glycoside substrate. On the other hand, the positive charge of amidine was supposed to induce a complementary negative charge, presumably a carboxylate, in the antibody binding site that could act as a proton donating group in glycoside hydrolysis. Actually, anti-amidine antibodies strongly bind haptens with positive charges suggesting the presence of a negative group in the binding site. However, examination of ionic pair interaction in various proteins between amidine or arginine group and an aspartate or a glutamate group have revealed that this interaction lies preferentially in the plane formed by the NH-C(R)-NH bonds.<sup>21</sup> Consequently, if anti-amidine antibodies have a carboxylate group in the binding site, it would not be in the right position to protonate the exocyclic oxygen during glycoside hydrolysis. These reasons tentatively explain why anti-amidine antibodies failed to catalyze glycoside hydrolysis. Present studies emphasize that potent inhibitors are not necessarily good transition state analogues and suggest that strong binding of mannoamidines to mannosidase is dominated by electrostatic interactions instead of geometric features such as the half chair conformation of the amidine ring. Our recent kinetic studies of benzylmannoamidines have shown that there is an energetic contribution of -2.8 kcal/mol from charge interaction.<sup>2b</sup> In addition, amino-sugars as isofagomine with a chair like conformation and a positive protonated amino group at the C-1' position have been recently synthesized and proved to be more potent glycosidase inhibitors.<sup>22</sup>

## MATERIAL AND METHODS

**Nomenclature.** The labelling of atoms and torsion angles of interest are represented on Fig. 2. The torsion angles which describe the conformation about the amidine linkage are  $\phi$ ,  $\psi$  and  $\omega$ , whereas those describing the orientation of the primary hydroxyl group are  $\chi$ . The orientations of the primary hydroxyl group are also referred to as either *gauche-gauche* (GG), *gauche-trans* (GT), or *trans-gauche* (TG). In this terminology the first and second terms characterise the torsion angles N-5'-C-5'-C-6'-O-6' and C-4'-C-5'-C-6'-O-6' respectively.

**NMR spectroscopy.**  $^1\text{H}$  (400.13 MHz) spectra were recorded with a Bruker ARX 400 instrument operating in the Fourier-Transform mode at 296 K. The  $^3\text{J}_{\text{H-H}}$  coupling constants were obtained from spectra acquired with 0.1 Hz digital resolution. Assignments of the  $^1\text{H}$  signals of benzyl mannoamidine **1** and pseudo (1 $\rightarrow$ 6) disaccharide **2** were obtained from the COSY spectra. Phase-sensitive NOESY spectra were acquired with mixing times of 800 ms.  $512 \times 1\text{K}$  data matrices were obtained and zero-filled to  $1\text{K}$

× 1K. A  $\pi/2$ -shifted sine-squared weighting function was applied prior to Fourier transformation.

**Computational methods.** The conformational analysis was performed using AM1 semi-empirical calculations either with a MOPAC 6.0 program (Proquantum software, Biostructure) on a Silicon Graphics Indigo or with Hyperchem 4.0 software (Hypercube, Inc., 419 Phillip Street, Waterloo, Ontario) on a Packard-Bell 486DX33 computer. All the calculations were done at the RHF level with a convergence limit of 0.01 kcal/mol. "Rigid" map calculations were calculated as a function of  $\psi$  and  $\omega$  at intervals of  $10^\circ$  with the hydroxymethyl group fixed in the more stable *GT* conformation. Iso-energy contours are drawn at intervals of 1 kcal/mol with respect to the observed energy minimum of each map. Each of the low energy conformers detected on the "rigid" potential energy surface is fully optimized. For each conformation, possible hydrogen bonds were identified using a criterion based on the distance (distance between donor hydrogen and acceptor atom less than 3.2 Å) and the angle made by the covalent bond to the donor and acceptor atoms (greater than  $150^\circ$ ).

$^3J_{\text{H-H}}$  coupling constants in the amidine ring were calculated using the Altona and Haasnoot equation.<sup>12</sup>

Partial atomic charges were obtained by MNDO semi-empirical calculations. Whereas PM3 and AM1 have been shown to be poor methods for providing atomic charges, MNDO is well recognized to give atomic charges similar to those obtained with *ab initio* methods.

Initial searches for transition states of glycoside hydrolysis were carried out by reaction coordinate methods. Thus, after protonation of the exocyclic O of glycoside, the C-O bond length was incremented by 0.2 Å and the AM1 enthalpy of formation determined. The structure located in this way close to the energy maximum was then further refined using TS subroutine of Spartan.<sup>23</sup> Finally, the transition structures were characterized by only one negative force constant.<sup>24</sup>

## ACKNOWLEDGMENTS

We thank the Ministère de la Recherche et de l'Enseignement Supérieur (MRES) for the fellowship granted to Y.B and A.G-G. We also thank Dr J.Y. Le Questel for performing the transition state calculations on Spartan.

## REFERENCES

1. a) M.K. Tong, G. Papandreou, and B. Ganem, *J. Am. Chem. Soc.*, **112**, 6137 (1990); b) B. Ganem and G. Papandreou, *J. Am. Chem. Soc.*, **113**, 8984 (1991); c) G. Papandreou, M.K. Tong and B. Ganem, *J. Am. Chem. Soc.*, **115**, 11682 (1993).



2. a) Y.T. Pan, G.P. Kaushal, G. Papandreou, B. Ganem and A.D. Elbein, *J. Biol. Chem.*, **267**, 8313 (1992); b) Y. Blériot, T. Dintinger, A. Genre-Grandpierre, M. Padrines and C. Tellier, *Bioorg. Med. Chem. Lett.*, **5**, 2655 (1995).
3. a) M.L. Sinnott, *Chem. Rev.*, **90**, 1171 (1990); b) G. Legler, *Adv. Carbohydr. Chem. Biochem.* **48**, 319 (1990).
4. J. Yu, L.C. Hsieh, L. Kochersperger, S. Yonkovich, J. Stephans, M.A. Gallop and P.G. Schultz, *Angew. Chem. Int. Ed. Engl.*, **33**, 339 (1994).
5. R.A. Lerner, S.J. Benkovic and P.G. Schultz, *Science*, **252**, 659 (1995) and references cited.
6. Y. Blériot, A. Genre-Grandpierre, and C. Tellier, *Tetrahedron Lett.*, **35**, 1867 (1994).
7. Y. Blériot, T. Dintinger, N. Guillo and C. Tellier, *Tetrahedron Lett.*, **36**, 5175 (1995).
8. M.J.S. Dewar, E.G. Zebisch, E.F. Healy and J.P.P. Stewart, *J. Am. Chem. Soc.*, **107**, 3902 (1985).
9. Y. Blériot, PhD Thesis, Nantes, France (1994).
10. J. Oszczapowicz, in *The Chemistry of Amidines and Imidates*, S. Patai and Z. Rappoport, Eds., Wiley, New York (1991).
11. C.L. Perrin, in *The Chemistry of Amidines and Imidates*, S. Patai and Z. Rappoport, Eds., Wiley, New York (1991).
12. C.A.G. Haasnoot, F.A.A.M. De Leeuw and C. Altona, *Tetrahedron*, **36**, 2783 (1980).
13. a) I. Tvaroska and J-P. Craver, *J. Chem. Res.*, Miniprint, 123 (1991); b) S.E. Barrows, F.J. Dulles, C.J. Cramer, A.D. French and D.G. Truhlar, *Carbohydr. Res.*, **276**, 219 (1995).
14. C. Hervé du Penhoat, A. Imberty, N. Roques, V. Michon, J. Mentech, G. Descotes and S. Pérez, *J. Am. Chem. Soc.*, **113**, 3720 (1991).
15. A. Imberty, S. Gerber, V. Tran and S. Pérez, *Glycoconjugate J.*, **7**, 27 (1990).
16. A. Imberty, V. Tran and S. Pérez, *J. Comput. Chem.*, **11**, 205 (1989).
17. P.A. Bartlett and C.K. Marlowe, *Biochemistry*, **22**, 4618 (1983).
18. M.A. Phillips, A.P. Kaplan, W.J. Rutter and P.A. Bartlett, *Biochemistry*, **31**, 959 (1992).
19. P. Ermert, A. Vasella, M. Weber, K. Rupitz and S. Withers, *Carbohydr. Res.*, **250**, 113 (1993).
20. R.J. Woods, C. W. Andrews and P. Bowen, *J. Am. Chem. Soc.*, **114**, 859 (1992).
21. *Atlas of Protein Side Chain Interaction*, J. Singh and J.M. Thornton, Eds., IRL Press, Oxford (1992).
22. T.M. Jespersen, M. Bols, M.R. Sierks and T. Skrydstrup, *Tetrahedron*, **50**, 13449 (1994).
23. Spartan 4.0, Wavefunction, Inc., 18401 Von Karman Ave, #370, Irvine, CA 92715, USA.
24. P. Deslongchamps, Y.L. Dory and S. Li, *Can. J. Chem.*, **72**, 2021 (1994).